A LABORATORY ANALOGUE FOR CLOUD ENTRAINMENT: WHOLE-FIELD VELOCITY AND TEMPERATURE MEASUREMENTS IN A VOLUMETRICALLY HEATED JET

Amit Agrawal
126 Spencer Lab, Department of Mechanical Engineering,
University of Delaware, DE 19716, USA
agrawaa@me.udel.edu

Ajay K. Prasad
126 Spencer Lab, Department of Mechanical Engineering,
University of Delaware, DE 19716, USA
prasad@me.udel.edu

ABSTRACT

Whole-field velocity and temperature measurements were conducted in the axial plane of an axisymmetric turbulent jet to investigate the effect of off-source volumetric heat addition on entrainment in clouds. The jet fluid was selectively heated while the ambient fluid temperature remained unaffected, simulating condensation heat release in clouds. Measurements in the heat injection zone are presented for varying Reynolds number and non-dimensional heat injection rate. Off-source heat addition causes the jet velocity to decay less rapidly, and the characteristic gaussian profile of the streamwise velocity is distorted to a "flat-top" gaussian. The cross-stream velocity experiences an even greater difference: the heated jet shows an inward velocity at *all* radial positions in the heating zone, in contrast to the outward velocity in the vicinity of the centerline for an unheated jet. These differences are linked to the different decay rates of the axial velocity of heated and unheated jets. The ensemble-averaged temperature exhibits an interesting double-peak. Further, the heat injection zone can be divided into three sub-zones with sharp differences in flow properties. A theoretical model incorporating the varying decay rates is proposed.

INTRODUCTION

Jets are examples of free-shear flows. Understanding them is critical because often more complex phenomena of combustion, aeroacoustics, propulsion and cloud-formation are modeled after these 'simple' flows.

Morton et al. (1956) first proposed that for free-shear flows in the self-similar regime, the mean entrainment velocity can be related to some characteristic velocity in the flow. The proportionality constant is called the coefficient of entrainment. While this model has been successfully applied to several flow situations (Turner 1986), it has been found that for cumulus clouds which have an off-source buoyancy addition, the model of Morton et al. (1956) is not strictly applicable. Upon heat release (due to condensation in clouds) the spreading of the rising plume is arrested (see for example, Scorer 1972), and the lateral entrainment is reduced (Paluch 1979). Warner (1970) shows that the lateral entrainment model for plumes cannot simulatneously predict the height of ascent and air-water ratio in cumulus clouds.

Elavarasan et al. (1995) and Bhat and Narasimha (1996) have replicated some of these features of clouds (reduction in the spread rate) in a laboratory by adding off-source volumetric heat to an axisymmetric jet. Sreenivas and Prasad (2000) have identified the difference in temperature gradient with and without heating as the key parameter to explain the increase in entrainment rate with buoyancy addition at the source (plumes versus jets), in contrast to reduced entrainment with off-source buoyancy addition (volumetrically heated jets versus normal jets).

Bhat and Narasimha (1996) show that with off-source heating, the divergence angle of the jet reduces. They find that the coherent structures in the jet are disrupted by heating. Their model (using a constant ratio of scalar and ve-

locity widths) shows that the increase in mass flux with downstream distance is much less for heated jets than their unheated counterparts, suggesting that entrainment is reduced with off-source heating. Elavarasan et al. (1995) measured an increase in volume flux in the heating zone – higher the heating rate, greater is the increase – in contradiction with the conclusions of Bhat and Narasimha (1996). However in the post-heating zone, Elavarasan et al. (1995) find a slightly smaller increment in the mass-flux with axial coordinate, as compared to normal jets.

In this paper results are presented for different non-dimensional heating rates, and are compared against normal unheated jets. To quantify the effect of heat, the non-dimensional heating number, G (Bhat and Narasimha 1996) and Re are used as appropriate.

$$G = \frac{\alpha g}{\rho C_p} \frac{z_b^2}{d^3} \frac{Q}{U_0^3}$$

where α is the coefficient of thermal expansion, g is acceleration due to gravity, ρ is the density of the unheated fluid, C_p is the specific heat at constant pressure, z_b is the axial distance from the nozzle where heating starts, d is the nozzle diameter, Q is the total power added to the jet, and, U_0 is the nozzle exit velocity. These measurements lead to a new understanding into the effect of variation of decay rates of the centerline velocity with downstream distance for free-shear flows.

EXPERIMENTAL PROCEDURE

Details of the jet facility employed for these experiments are given by Agrawal and Prasad (2001b). The jet fluid was volumetrically heated in an off-source manner, using a scheme developed by Bhat et al. (1989). In this method, differences in water conductivity are used to selectively heat the jet fluid. The body of the jet is made conducting by adding hydrochloric acid to it (~15ml of HCl/l of water), whereas the ambient fluid in the tank is filled with deionized water which is non-conducting (Fig. 1). Densities of the jet and ambient water are matched by adding appropriate amount of acetone to the jet fluid. When the jet is operating, only that portion of the jet body present between multiple wire-grids conducts electricity resulting in ohmic heating, thus simulating the latent heat release in clouds due to condensation or freezing. These experiments are characterized by short run times (3-5 min).

150μm stainless steel wires on 1cm square grid are used for heating the jet. We have used 6 grids spaced 2.5cm vertically, with alternate ones connected to opposite terminals of a high power, high frequency power amplifier (1200W at 20kHz). Power into the jet is calculated knowing the voltage and current across the grids.

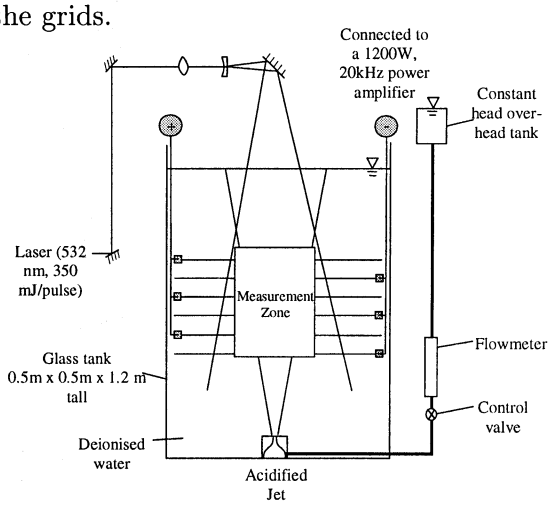

Figure 1: Experimental set-up

Twin Nd-YAG pulse lasers (350 mJ/pulse at 532nm) provide illumination for PIV. 20-40μm fluorescent particles are used as tracers for PIV. Images are recorded at 0.5Hz using a Kodak 1.0 ES CCD camera with a 1026 $\times$ 1000 pixels array. A long-wave filter is used to eliminate elastic scattering from the grids.

Temperature measurements are accomplished using a dilute suspension of micro-encapsulated thermochromic liquid crystals (TLC) as temperature sensors. The different colors reflected by the crystals are calibrated versus temperature. The crystals used here are active in a 3.3 C bandwidth (23.5-26.8 C). An axial plane is illuminated with white light, and images are recorded at 2Hz using a color CCD camera (DVC, with a 1300 $\times$ 1030 pixels array). At this stage, our results for temperature are rather preliminary; nevertheless they contribute significantly to our understanding.

RESULTS

Unheated Jets (baseline)

Both LIF and PIV results are virtually identical with and without grids, confirming that the grids are not affecting the flow. Values of important parameters were obtained by PIV measurements without the grids and were found in good agreement with previous researchers (Turner 1986). For example, the spread rate, db/dz was found as $c = 0.11$ (here, b is defined using $U(b)/U_c = e^{-1}$).

As expected the streamwise velocity profile ($110 \leq z/d \leq 175$) was found to be a gaussian (Agrawal and Prasad 2001b). The cross-stream velocity is small but matches well with the theoretical profile (Fig. 2; deviation at large r/b could be due to the finite size of the tank). It was verified that the centerline velocity decays as z^{-1} in agreement with the results of similarity analysis for axisymmetric jets. For a small control volume (CV) centered at the axis, the decay in the centerline velocity with downstream distance causes the axial volume flux to decrease. The excess volume exits the lateral sides of the CV resulting in a volume outflow near the jet axis. However, for a CV extending to large r/b (and therefore encompassing the entire jet) a net increment in volume with axial coordinate, causes the lateral volume flux to point towards the axis (Agrawal and Prasad 2001a).

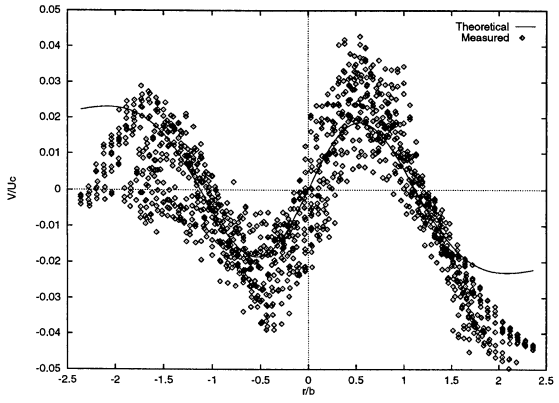

Figure 2: Measured versus theoretical cross-stream velocity profile for baseline (unheated) jet.

Volumetrically Heated Jets

Heating Zone.

Figure 3 shows an example of a TLC image (Re=1450, $202 \leq z/d \leq 267$, $\approx$4 min from start). It is apparent that the jet fluid is indeed getting selectively heated. The ambient is at 23.5 C (red), while the jet fluid changes from the ambient color near the bottom of the frame to blue near the top, i.e., the temperature of the jet increases with the axial coordinate.

One can make several important observations by comparing the jet before the second grid (in the frame) versus the jet downstream of this grid location. For example, the narrowing of the jet is apparent beyond the second grid; also large eddies are observed upto this axial location and are less apparent beyond it. Beyond the second grid, the jet appears to be getting axially stretched and relaminarized. Evidence points to a critical temperature beyond which the transition (sudden change in spread rate, etc.) occur.

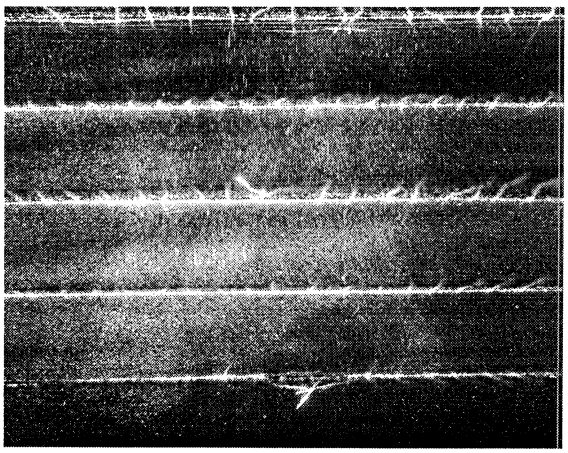

Figure 3: Temperature visualization in a heated jet with TLC (red = cold, blue = hot).

Reduction in the spread rate with heat was confirmed by time-averaging individual LIF realizations. Disruption of the large eddies might partly be the reason for the observed decrease in the spread rate.

For PIV measurements, the heated zone extends between $200 \leq z/d \leq 265$ (Re=2400, G=5.4). The view-frame between $200 \leq z/d \leq 289$ includes and extends slightly beyond the heating zone. Along the lines of the visual observations described above, it is possible to identify three distinct regions located axially in the heated zone. Here, we have used the cross-stream velocity profiles to demarcate these 3 regions. The streamwise and cross-stream velocity (in cm/s) profile for these regions are presented in Figs. 4 and 5 respectively (averaged from 337 statistically independent frames).

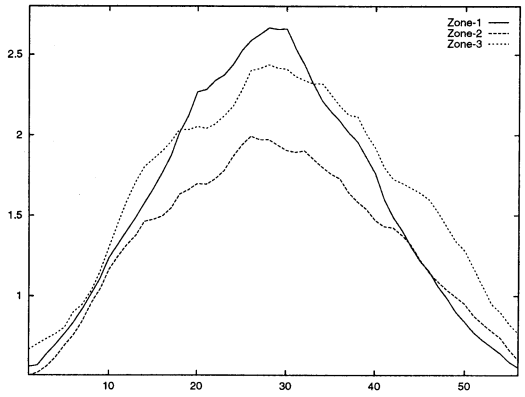

Figure 4: Streamwise velocity for different zones.

In the lower zone (zone-1), the effect of heat is barely noticeable – the streamwise velocity is still gaussian in nature (Fig. 4); the cross-

stream velocity profile exhibits positive and negative values (Fig. 5) that closely resemble the baseline, unheated case.

In the middle zone (zone-2), the effect of heat is apparent from the change in the cross-stream velocity profile. The cross-stream velocity is nearly zero for all r in the viewing zone (Fig. 5). (Despite large fluctuations in the profile the mean is nearly zero.) In contrast to unheated jets, regions of mass influx or outflux are not observed for the radial extent covered by the view-frame (Fig. 5).

In the upper zone (zone-3), the effect of heat is most strongly visible. The streamwise velocity profile changes from a normal gaussian to a gaussian profile with a flattened top (Fig. 4). For this zone, the cross-stream velocity profile shows a remarkable deviation from a normal jet profile. As can be readily seen from Fig. 5, the cross-stream velocity, V is *negative* for small r and tends to 0 further out, i.e., a mass inflow is seen for all r in this zone. Note, V cannot become positive for r beyond the view-frame, as that would violate continuity.

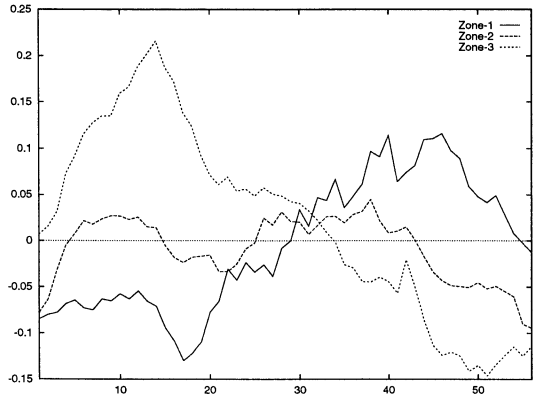

Figure 5: Cross-stream velocity for different zones.

Figure 6 compares the variation of centerline velocity, with downstream distance for a heated versus an unheated axisymmetric jet. ($1/U_c$ is plotted for a easier comparison with the unheated jet.) It is seen that U_c initially decreases and then increases. Decrease in U_c indicates deceleration and corresponds to a slightly wider than normal jet; however, as heat starts to affect the jet, the decay of U_c is arrested (zone-2). Finally, due to addition of heat the jet starts to accelerate (zone-3). The coupling between decay rate and volume outflow can be understood in view of the recent work of Agrawal and Prasad (2001a). For example, the decay rates of axisymmetric jets, planar jets, and axisymmetric plumes are respectively $z^{-1}, z^{-1/2}, z^{-1/3}$, while the radial extents of outflow are $r/b \leq 1.12, 0.99, 0.59$. Moreover, the decay rate for planar plumes varies as z^0 and these do not experience any outflow, i.e., a higher decay rate correlates with a larger radial extent of outflow. A similar argument indicates that a decrease in the decay rate leads to a smaller radial extent of outflow. Eventually an accelerating jet will experience a pure inflow towards the jet axis for all r. Therefore, the results of Figs. 5 and 6 are consistent with the theoretical results of Agrawal and Prasad (2001a).

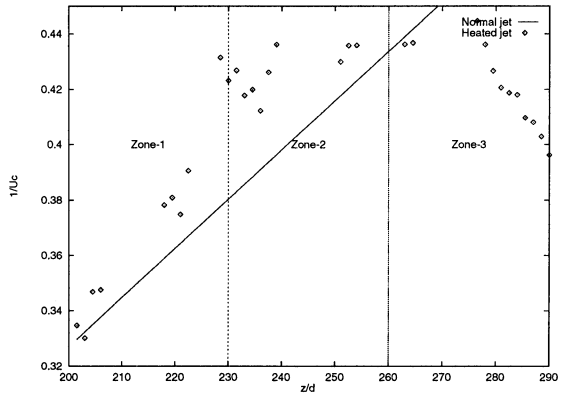

Figure 6: Centerline velocity for heated and normal jet.

The width of the jet as a function of the downstream coordinate is plotted in Fig. 7. The result is in *contrast* with the scalar width result – the velocity width for the heated jet is larger than the unheated jet. Moreover, the velocity width of the jet increases in the initial part of the heat injection zone, and then remains constant or decreases with z. The momentum of the jet has to increase due to buoyancy addition. However, because U_c seems to decrease faster than z^{-1}, the width has to increase over and above that for a normal jet. Subsequent decrease in velocity width might be linked to a decrease in the scalar width or to stable stratification (Sreenivas and Prasad 2000).

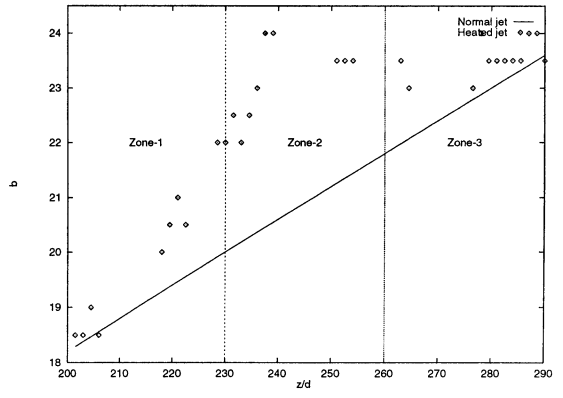

Figure 7: Velocity width for heated and normal jet.

Referring back to the temperature visualiza-

tion in Fig. 3, it can be seen that for a given axial location upstream of the fourth grid, the temperature increases with radial position. This can be expected because (for gaussian velocity and scalar distributions) the fluid near the centerline carries the most acid but has the smallest residence time in the heat injection zone; similarly, near the jet edge the fluid has a large residence time but a small acid concentration. Assuming that the amount of heating is directly proportional to the acid concentration, it can be argued that the maximum temperature rise may occur away from the centerline. This is confirmed by time-averaging the individual temperature fields between the third

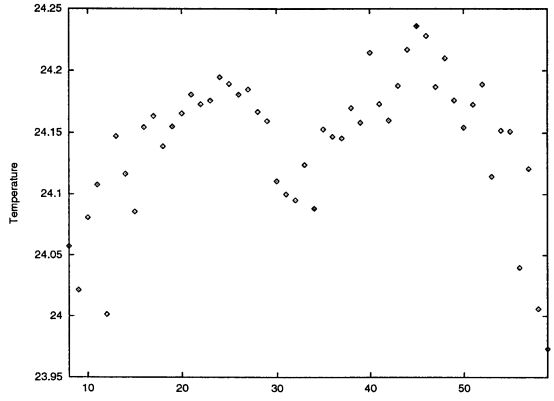

Figure 8: Temperature for $241 \leq z/d \leq 245$.

and fourth grids (Fig. 8, $241 \leq z/d \leq 245$) – although the average (of 172 frames) maximum temperature rise is small (less than a degree) the twin peaks can be clearly discerned. For $257 \leq z/d \leq 263$, the time-averaged temperature is shown in Fig. 9. The temperature profile looks like a flat-top gaussian. The difference in the temperature profiles for the two axial locations could result because for the former, the velocity profile is a gaussian (zone-2), while the latter has changed to a flat-top gaussian (zone-3). It can be similarly argued that for a flat-top gaussian velocity profile with either a gaussian or a flat-top gaussian distribution for acid concentration, the temperature rise will be maximum at the centerline, and the resulting temperature profile will more closely resemble a flat-top gaussian than a gaussian.

Variation in heating rates.

Besides Re, G was also varied for this study ($0 \leq G \leq 16$ is used in this investigation). The jet passes through the heating zone almost unaffected for small values of G. However as G increases, the spread rate decreases. The jet rises like a column and even converges (instead of diverging) for still higher values of G.

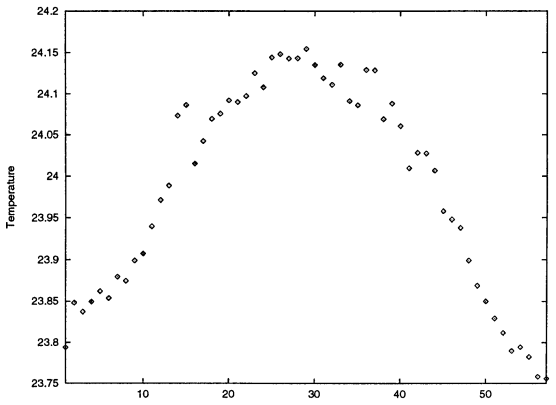

Figure 9: Temperature for $257 \leq z/d \leq 263$.

These observations are consistent with Bhat and Narasimha (1996).

Moreover, we find that with higher G, the second and third zones moves closer to z_b. This is expected as the jet feels the effect of heat more strongly as G increases. The transition from a pure gaussian to a flattened gaussian (zone-3) is not apparent for lower G, however, as G increases the flat top becomes very pronounced.

DISCUSSION

Theoretical model for the heated jet

We have found that the streamwise velocity for the heated jet (in zones 2 and 3) can be well represented by:

$$U = \frac{U_c}{z^n}\left(1 + \frac{Br^2}{c^2 z^2}\right)\exp\left(-\frac{r^2}{c^2 z^2}\right) \qquad (1)$$

where, n characterizes the decay rate of the centerline velocity, and, B is the flatness factor for the "flat-top" gaussian (flatness increases with B). It should be noted that for $n = -1, B = 0$ a reduction to a gaussian profile is obtained. The effect of heat is to make the velocity decay less rapidly, i.e., make $n > -1$, and distort the gaussian to a flat top ($B > 0$). (We expect $B \leq 1$, because $B > 1$ gives double peaks which are not observed experimentally.) Thus, while n reflects the effect of heat in the axial direction, B captures the radial effect of heat.

Further, it can be seen that on subtracting a gaussian from Eq. 1 the resulting profile has twin peaks, and it resembles the temperature profile (in Fig. 8) quite closely (Fig. 10). In other words, the net effect of heat on the jet is a twin peaked profile (obtained from buoyancy addition) superimposed on the normal gaussian (for a normal jet), resulting in a flat-top

gaussian profile for velocity. This flat-top velocity profile will in-turn change the twin peak gaussian for temperature (at $z/d = 243$) to a flat-top (at $z/d = 260$).

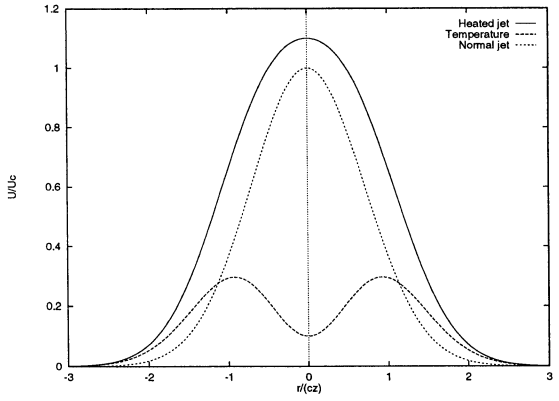

Figure 10: Effect of heat on the streamwise velocity.

The continuity equation (with Eq. 1) can be solved to yield the cross-stream velocity, V for the volumetrically heated jet. A sample result for V corresponding to $n = 0$ and $B = 1/2$ is:

$$\frac{V}{U_c} = c\left(\exp\left(-\frac{r^2}{c^2z^2}\right)\frac{3+\frac{3r^2}{c^2z^2}+\frac{r^4}{c^4z^4}}{\frac{2r}{cz}} - \frac{3}{\frac{2r}{cz}}\right)$$

Results for (B=0, n=-1), (B=1/2, n=0), and (B=2/3, n=1/2) are plotted in Fig. 11. These can be seen to capture the trend of the cross-stream velocity profile in Fig. 5 quite well.

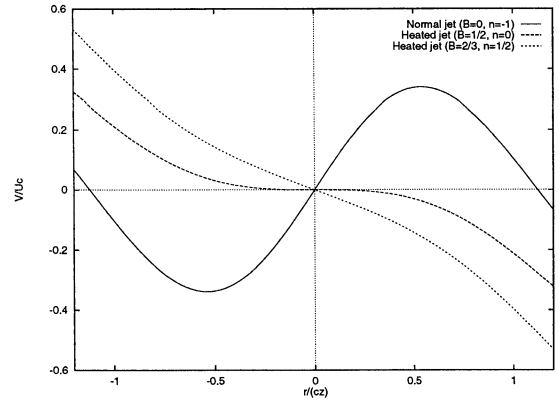

Figure 11: Effect of heat on the cross-stream velocity.

The ratio of momentum carried by an axisymmetric jet with the velocity profile given by Eq. 1 to that of a normal jet, is given by:

$$\frac{M_{\text{heated}}}{M_{\text{normal}}} = \frac{1+(1+B)^2}{2}$$

As expected, for the same jet width and centerline velocity, momentum transported by the heated jet profile is larger than for a jet with a gaussian velocity profile. This might partly be a reason for the change from gaussian to a flat-top gaussian with heating.

Similarly, for the same centerline velocity and jet width, the ratio of the mass fluxes for the heated versus a normal jet can be obtained as:

$$\frac{\mu_{\text{heated}}}{\mu_{\text{normal}}} = 1 + B$$

i.e., the volume flux for a heated jet is $(1+B)$ times larger than a normal jet.

Acknowledgements

This work was supported by National Science Foundation, under grant NSF-ATM-9714810.

References

Agrawal, A., and Prasad, A.K., 2001a, "Derivation of time-averaged flow-profiles for turbulent jets, plumes and wakes," in review, *AIAA J.*

Agrawal, A., and Prasad, A.K., 2001b, "Coherent structures in the self-similar turbulent jet," in review, *Phy. Fluids.*

Bhat, G.S. and Narasimha, R., 1996, "A volumetrically heated jet: large eddy structure and entrainment characteristics," *J. Fluid Mech.,* Vol. 325, pp. 303-330.

Bhat, G.S., Narasimha, R., and Arakeri, V.H., 1989, "A new method of producing local enhancement of buoyancy in liquid flows," *Exp. Fluids,* Vol. 7, pp. 99-102.

Elavarasan, R., Bhat, G.S., Narasimha, R., and Prabhu, A., 1995, "An experimental study of a jet with local buoyancy enhancement," *Fluid Dyn. Res.,* Vol. 16, pp. 189-202.

Morton, B.R., Taylor, G.I., and Turner, J.S., 1956, "Turbulent gravitational convection from maintained and instantaneous sources," *Proc. R. Soc. London,* Ser. A, Vol. 234, pp. 1-23.

Paluch, I.R., 1979, "The entrainment mechanism in Colorado cumuli," *J. Atmos. Sci.,* Vol. 36, pp. 2467-2478.

Scorer, R.S., *Clouds of the world - A complete color encyclopedia,* 1972, Lothian Pub. Co.

Sreenivas, K.R., and Prasad, A.K., 2000, "Vortex-dynamics model for entrainment in jets and plumes," *Phys. Fluids,* Vol. 12, pp. 2101-2107.

Turner, J.S., 1986, "Turbulent entrainment: the development of the entrainment assumption, and its application to geophysical flows," *J. Fluid Mech.,* Vol. 173, pp. 431-471.

Warner, J., 1970, "On steady-state one-dimensional models of cumulus convections," *J. Atmos. Sci.,* 27, pp. 1035-1040.